

Basolateral K Channels in an Insect Epithelium

Channel Density, Conductance, and Block by Barium

J. W. HANRAHAN, N. K. WILLS, J. E. PHILLIPS, and
S. A. LEWIS

From the Department of Physiology, Yale University School of Medicine, New Haven, Connecticut 06510, and the Department of Zoology, University of British Columbia, Vancouver, B.C., V6T 2A9 Canada

ABSTRACT K channels in the basolateral membrane of insect hindgut were studied using current fluctuation analysis and microelectrodes. Locust recta were mounted in Ussing-type chambers containing Cl-free saline and cyclic AMP (cAMP). A transepithelial K current was induced by raising serosal [K] under short-circuit conditions. Adding Ba to the mucosal (luminal) side under these conditions had no effect; however, serosal Ba reversibly inhibited the short-circuit current (I_{sc}), increased transepithelial resistance (R_t), and added a Lorentzian component to power density spectra of the I_{sc} . A nonlinear relationship between corner frequency and serosal [Ba] was observed, which suggests that the rate constant for Ba association with basolateral channels increased as [Ba] was elevated. Microelectrode experiments revealed that the basolateral membrane hyperpolarized when Ba was added: this change in membrane potential could explain the nonlinearity of the $2\pi f_c$ vs. [Ba] relationship if external Ba sensed about three-quarters of the basolateral membrane field. Conventional microelectrodes were used to determine the correspondence between transepithelially measured current noise and basolateral membrane conductance fluctuations, and ion-sensitive microelectrodes were used to measure intracellular K activity (a_k). From the relationship between the net electrochemical potential for K across the basolateral membrane and the single channel current calculated from noise analysis, we estimate that the conductance of basolateral K channels is ~ 60 pS, and that there are ~ 180 million channels per square centimeter of tissue area.

Address reprint requests to Dr. S. A. Lewis, Dept. of Physiology, Yale University School of Medicine, B-106 SHM, P.O. Box 333, New Haven, CT 06510-8026. Dr. Hanrahan's present address is Dept. of Physiology, McGill University, 3655 Drummond St., Montreal, P.Q., H3G 1Y6 Canada.

INTRODUCTION

Many epithelial cells in vertebrate and invertebrate animals have a large K conductance in their basolateral membrane that allows K ions entering through the Na/K pump to return to the serosal side (Koefoed-Johnsen and Ussing, 1958; reviewed by Lewis et al., 1984*b*). Basolateral K conductance influences the electrical potential across the apical membrane because of the finite conductance of the paracellular shunt, and is therefore important in determining flux through apical ion channels and electrogenic cotransporters (e.g., Morgunov and Boulpaep, 1984; Lapointe et al., 1984). In addition, basolateral K conductance has been implicated in the regulation of cell volume in several epithelia (Germann et al., 1984; Lau et al., 1984; Lewis et al., 1984*a*). While inhibition of basolateral K conductance by millimolar levels of Ba is well established in many epithelia, the kinetics and voltage dependence of Ba block have not been examined. In fact, relatively little is known about basolateral K conductance at the single channel level in absorptive epithelia, although exocrine glands have been studied using the patch-clamp technique (e.g., Maruyama et al., 1983*a, b*).

Current fluctuation analysis has been used extensively for studies of epithelial ion channels. By assuming a simple model for blocker interactions, noise analysis has allowed the calculation of single channel currents and the densities of apical Na and K channels (e.g., Lindemann and Van Driessche, 1977; Van Driessche and Zeiske, 1980). However, this approach has been less useful for studying basolateral channels because many preparations have a high apical membrane resistance, which leads to attenuation of transepithelial current noise relative to conductance fluctuations at the basolateral membrane. This problem can be minimized by using ionophores such as nystatin to lower apical membrane resistance artificially. For example, spontaneous current noise from the basolateral membrane has been measured under these conditions in rabbit colon (Wills et al., 1982; see Wills, 1984) and amphibian skin (Van Driessche et al., 1982). Nonetheless, it has not been possible so far to estimate basolateral single channel currents or their conductance, nor has the number of channels per unit tissue area been assessed in these epithelia.

One preparation that is uniquely suited for studying basolateral K channels by this technique is the hindgut of the desert locust. The locust renal system consists of Malpighian tubules, which actively secrete a K-rich primary urine (140–165 mM K) into the hindgut, and rectal pads that selectively reabsorb water, salts, and nutrients (see Phillips, 1981). Flat-sheet cable analysis has shown that the locust rectum is a tight epithelium, and that most of the K secreted by Malpighian tubules is recovered passively in the rectum through conductive pathways in the apical and basolateral membranes (Hanrahan and Phillips, 1984*b, c*). Furthermore, apical K conductance is under hormonal control in locust rectum, and can be stimulated fivefold by cAMP *in vitro* without affecting the K conductance of the basolateral membrane (Hanrahan and Phillips, 1984*b*).

In this paper, we exploit these unusual properties of insect hindgut to study basolateral K channels. cAMP-stimulated recta are short-circuited in the presence of a transepithelial K gradient, and Ba-induced fluctuations in I_{sc} are analyzed. We estimate the kinetics of block and the single channel current from transepi-

thelial noise, and use microelectrode data collected under identical conditions to correct for the attenuating effects of the apical membrane. The corrected single channel current is then used to calculate channel density and to determine channel conductance from Ba-induced variations in K driving force.

Some of these data were reported previously in abstract form (Hanrahan et al., 1983).

METHODS

Preparations

To measure transepithelial current noise, recta from adult male desert locusts (*Schistocerca gregaria*, Forskål) were dissected and mounted in Ussing-type chambers (Lewis and Diamond, 1976) modified to expose 0.239 cm² of tissue. Each half-chamber had a volume of 15 ml and was vigorously stirred and oxygenated except when records were actually being collected for analysis. Tissues were allowed to equilibrate for 30 min in normal saline containing (mM): 70 Na, 10 K, 10 Mg, 5 Ca, 110 Cl, 10 glucose, 100 sucrose, 10 proline, and 5 glutamine at pH 7.2. Based on previous studies of this tissue (Hanrahan and Phillips, 1984a-c), we optimized the experimental conditions for studying transcellular K current (see Fig. 1, A and B). First, Cl was replaced with gluconate on both sides to abolish electrogenic Cl absorption and basolateral Cl conductance. Second, 1 mM cAMP was added to the serosal side to stimulate apical membrane K conductance. Finally, a transcellular K current was induced by replacing serosal Na with K.

Under these short-circuit conditions, we would expect the chemical gradient across the basolateral membrane to be virtually eliminated and intracellular potential to result from the outward K gradient at the apical membrane. A serosal-to-mucosal (s → m) rather than a mucosal-to-serosal (m → s) K gradient was chosen because there is evidence that apical K permeability declines in the presence of high mucosal [K] (Hanrahan and Phillips, 1984a). To induce current fluctuations, we added 0–20 mM Ba(NO₃)₂ to the serosal side from a concentrated aqueous stock solution (200 mM). The same volume of 400 mM NaNO₃ was added to the mucosal side.

For intracellular recording, we used a microelectrode chamber that has been described in detail elsewhere (Hanrahan et al., 1984b; Hanrahan and Phillips, 1984a). Aside from the different chambers used, other experimental conditions during intracellular measurements were identical to those described above for noise analysis. Both chamber designs have been shown to cause minimal edge damage. All experiments were done at room temperature (~22°C).

Electrical Methods

A low-noise voltage clamp similar to the one described by Van Driessche and Lindemann (1978) was used to measure short-circuit current. Data collection and analyses were similar to those described previously (Loo et al., 1983; Lewis et al., 1984c; Wills et al., 1984). Briefly, electrodes (voltage-measuring and current-passing) were Ag/AgCl wires imbedded in 4% agar/1 M KCl. Voltage-sensing agar bridges were positioned as close to the tissue as possible and ~30° normal to the plane of the epithelium using micromanipulators. I_{sc} was recorded after high-pass-filtering at 0.03 Hz (113, EG&G Princeton Applied Research, Princeton, NJ), amplified, low-pass-filtered through a 20-pole Cauer-Elliptic filter set at 100 Hz to prevent aliasing (LP120, Unigon Industrial Inc., Mount Vernon, NY), and sampled every 5 ms. The resulting 32,768 points were fast-Fourier-transformed in blocks of 2,048, beginning after every 512th point. The final power spectra, which represent an average of 61 transforms obtained from 16 overlapping data blocks, were fitted using a

nonlinear curve-fitting routine based on the derivative-free Levenberg-Marquardt algorithm of Brown and Dennis (1972). Following Van Driessche and Zeiske (1980), spectra were fitted as the sum of linear and Lorentzian-type functions:

$$S_1(f) = A/f^\beta + S_1(0)/[1 + (f/f_c)^2], \quad (1)$$

where A is defined as the power at 1 Hz, β is the slope of the linear component, $S_1(0)$ is

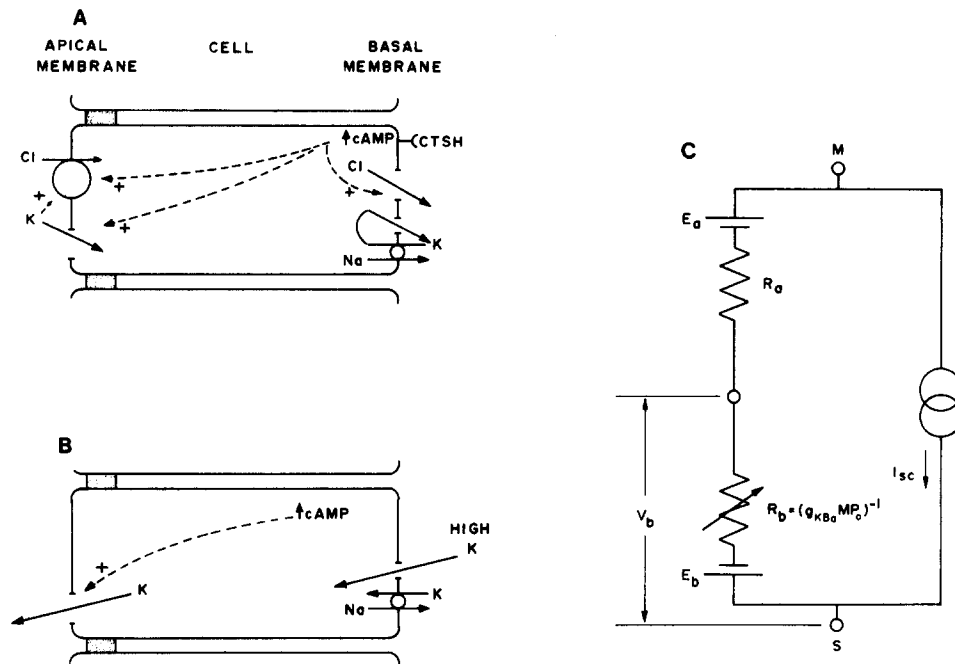


FIGURE 1. (A) Diagram of KCl transport across locust rectum bathed in normal saline containing 110 mM Na, 10 mM K, and 110 mM Cl. The peptide "chloride transport-stimulating hormone" (CTSH) elevates intracellular cAMP (Spring and Phillips, 1980). Cyclic AMP stimulates (a) apical K conductance, (b) active Cl influx, and (c) basolateral membrane Cl conductance (Hanrahan and Phillips, 1984). (B) Experimental conditions used to study basolateral K conductance. Cl was replaced with gluconate on both sides. Cyclic AMP (1 mM) was used to stimulate apical K conductance. $I_{K_{Ba}}$ was induced by raising serosal [K] from 10 to 80 mM. These conditions were designed to optimize basolateral membrane voltage clamp when V_i was short-circuited. (C) Equivalent circuit of locust rectum under the experimental conditions shown in B, including the voltage clamp. E_a and E_b are the emf's of apical and basolateral membranes, respectively, R_a is the resistance of the apical membrane, and R_b is the resistance of the basolateral membrane, which depends on [Ba]. $g_{K_{Ba}}$ is the single channel conductance, M is the number of channels, and P_o is the probability that a channel is unblocked. For simplicity, the high-resistance paracellular pathway and its emf have not been included: under short-circuit (I_{sc}) conditions, paracellular current would not flow through R_b and can be subtracted when calculating $I_{K_{Ba}}$ (see text). V_b is the basolateral membrane potential, which under short-circuit conditions is identical to the apical membrane potential.

the low-frequency plateau of the Lorentzian component, and f_c is the corner frequency. The macroscopic I_{sc} was monitored on a strip-chart recorder and digitized by a 12-bit A/D converter interfaced to a microcomputer (NorthStar Horizon II).

Single-barreled microelectrodes were pulled (PP-83, Narishige Scientific Instruments Laboratory, Tokyo, Japan) from borosilicate tubing containing a solid fiber (1.0 mm o.d., Frederick Haer & Co., Brunswick, ME). Conventional microelectrodes were filled with 0.5 M KCl and had resistances of $16.6 \pm 1.5 \text{ M}\Omega$. The tips of K-selective microelectrodes were silanized, filled with resin (477317, Corning Glassworks, Corning, NY), and back-filled with 0.5 M KCl as previously described (Hanrahan et al., 1984b; Hanrahan and Phillips, 1984b). Ion-sensitive microelectrodes were calibrated in solutions containing 1, 10, 50, and 100 mM KCl immediately before or after making a series of ~ 12 impalements. The electrodes used in the present experiments had a mean slope of $53.24 \pm 0.58 \text{ mV/decade}$ change in K activity ($\bar{x} \pm \text{SE}$, 33 electrodes), as calculated from the modified Debye-Hückel theory (Robinson and Stokes, 1959). No correction was made for interference by intracellular Na (a_{Na}^i) because electrodes were relatively selective for K over Na according to the separate solution method in which electrode emf's are compared in pure solutions (selectivity for K over Na = 62.4 ± 2.2), and because a_{Na}^i in locust rectal cells bathed with normal saline ($\sim 8 \text{ mM}$; Hanrahan and Phillips, 1984b) is normally too low to affect K activity measurements significantly. Moreover, a_{Na}^i is probably reduced further under the present high-K conditions.

Transepithelial potential (V_t) was arbitrarily clamped to 7 mV for 110 ms and the resulting deflections in apical (V_a) and basolateral membrane potentials (V_b) were recorded. We estimated α , the ratio of apical-to-basolateral membrane resistance (R_a/R_b), according to

$$\alpha = \Delta V_a / \Delta V_b \approx R_a / R_b. \quad (2)$$

The voltage drop caused by saline resistance between the voltage-sensing agar bridges and epithelium was subtracted when calculating α , R_t , and the net driving force for K across the basolateral membrane. The effect of mucosal saline resistance on ΔV_a was very small ($< 0.5 \text{ mV}$, barely detectable in Fig. 7 as deflections in the trace between impalements), although the saline resistance was somewhat larger on the serosal side and resulted in deflections of $\leq 1.6 \text{ mV}$.

Net electrochemical potential for K across the basolateral membrane ($\Delta \bar{\mu}_K^b / F$) was calculated as

$$\Delta \bar{\mu}_K^b / F = (RT/F) \ln(a_K^i / a_K^s) + V_b, \quad (3)$$

where a_K^i and a_K^s are intracellular and serosal K activities, respectively, and R , T , F , and V_b have their usual meanings. Statistical significance was determined using unpaired t tests.

Equivalent Circuit Model

Fig. 1C shows an equivalent circuit model for locust rectum, which is useful when interpreting the data presented below. We note the following features. (a) Apical membrane resistance (R_a) is minimized by adding cAMP (Hanrahan and Phillips, 1984b). (b) The [K] gradient from cell-to-mucosa (measured in Results) is largely responsible for E_a because apical Na conductance is negligible, and because both compartments are nominally Cl-free. (c) Junctional resistance (R_j) and the diffusion potential within the paracellular pathway (E_j ; caused by $s \rightarrow m$ K gradient and $m \rightarrow s$ Na gradient) are omitted from this simplified circuit. Locust rectum is a very tight epithelium during cAMP stimulation

according to cable analysis, so that little current would flow paracellularly (Hanrahan and Phillips, 1984b). Furthermore, paracellular current is excluded from subsequent calculations by subtracting the Ba-insensitive current (see below). (d) A basolateral membrane emf (approximately -5 mV) is included because the basolateral K gradient was not completely abolished under our experimental conditions (see Results). (e) Basolateral membrane conductance is shown as a variable resistor that depends on the Ba concentration. (f) The saline resistance between voltage-sensing agar bridges and the epithelium is not included; however, series resistance was minimized during noise experiments by positioning the agar bridges very close to the tissue using micromanipulators, and corrected for in microelectrode experiments as described above.

RESULTS

Effects of Serosal Ba on I_{sc}

When recta were mounted in Ussing-type chambers under control, open-circuit conditions, V_t decreased during the first hour from 16.6 ± 2.5 to 4.7 ± 1.8 mV ($\bar{x} \pm$ SE, 11 recta), results comparable to those obtained previously using a similar saline (Hanrahan and Phillips, 1984a). Fig. 2A shows the effect on V_t of increasing

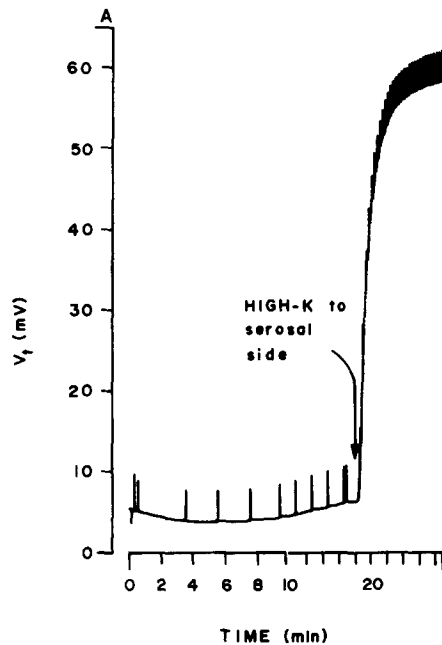


FIGURE 2. (A) Effect of raising serosal K concentration from 10 to 80 mM under open-circuit conditions (V_t referenced to the serosal solution). Both sides were nominally Cl-free (gluconate-substituted) and 1 mM cAMP was present on the serosal side. Brief deflections in the trace result from constant-current pulses (1.8 μ A), which were used to monitor tissue resistance. Preparation LOC0122. (B) Effect of serosal Ba on short-circuit current (I_{sc}). Most I_{sc} was Ba sensitive. Deflections in I_{sc} became smaller when Ba was added, which indicated an increase in transepithelial resistance (R_t). Preparation LOC0907. (C) Effect of Ba on the macroscopic K current ($I_{K_{Ba}}$; Ba-insensitive current subtracted) and R_t . Mean \pm SE.

serosal K concentration from 10 to 80 mM in the presence of 1 mM cAMP under Cl-free conditions. When V_t was clamped to 0 mV, the mean I_{sc} was variable ($53.9 \pm 11.0 \mu A cm^{-2}$); however, most of the current was abolished by adding Ba to the serosal side (Fig. 2B). We did not observe a gradual increase in I_{sc} after prolonged exposure to Ba like that described in frog skin (Van Driessche

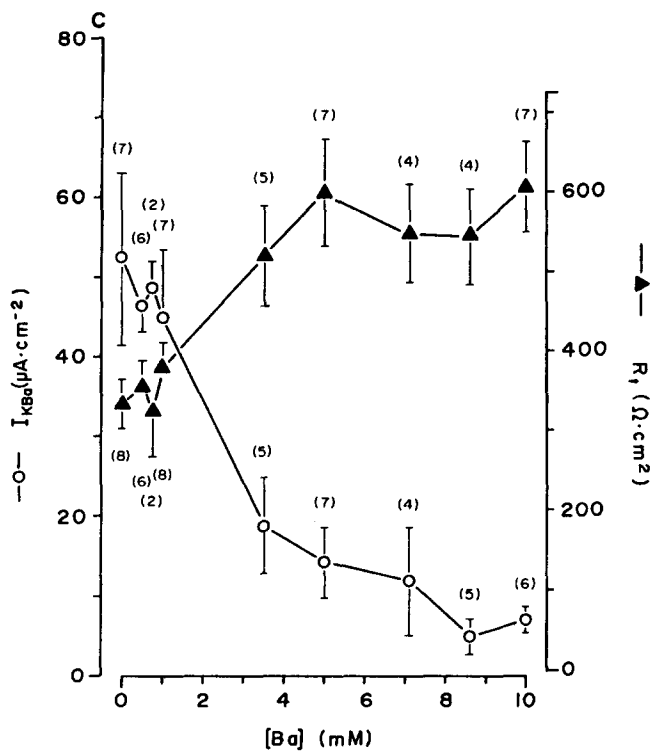
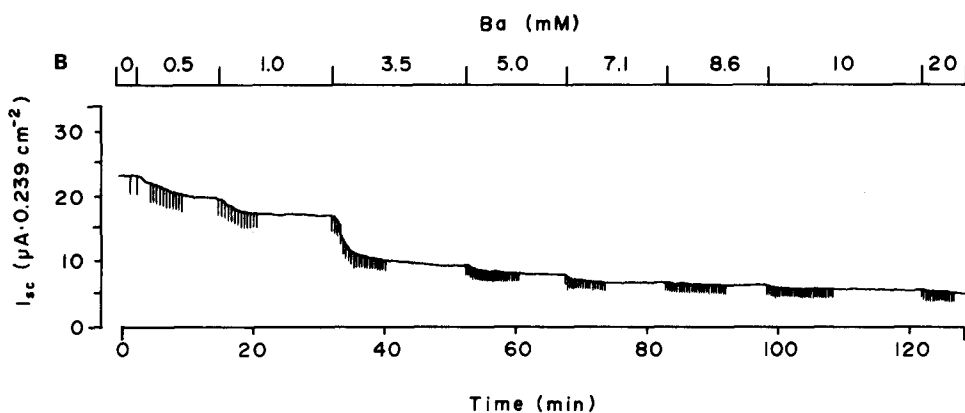


FIGURE 2, B and C

and Zeiske, 1980). However, there was often a small decline in transepithelial resistance when serosal $[\text{Ba}(\text{NO}_3)_2]$ was elevated beyond 10 mM, probably a consequence of nitrate conductance. To minimize this problem, only data obtained at low Ba concentrations (≤ 10 mM) were used when calculating the blocking kinetics and channel properties.

We obtained I_{KBa} , the macroscopic current flowing through Ba-sensitive channels, at each Ba concentration by subtracting the I_{sc} observed with 20 mM or 13.1 mM Ba present on the serosal side from that measured; i.e.,

$$I_{\text{KBa}} = I_{\text{sc}} - I_{\text{R}}, \quad (4)$$

where I_{R} is the residual current remaining when all the Ba-sensitive channels are blocked. Fig. 2C shows the decline in I_{KBa} and the increase in R_{t} caused by adding Ba to the serosal side. Half-maximal inhibition of I_{KBa} (i.e., the macroscopic K_{i}) appears to be in the range of 2.0–3.0 mM Ba, which is similar to that reported for external Ba block in other cells (e.g., squid axon; Armstrong et al., 1982).

Ensemble Analysis of Ba-induced Current Fluctuations

Adding millimolar levels of barium to the serosal (high-K) solution induced fluctuations in the short-circuit current (5 mM Ba; Fig. 3A), which decreased at very high Ba concentrations (20 mM). In the complete absence of Ba ("control"; Fig. 3B) or when Ba was added only to the mucosal side, the power spectral density of the I_{sc} noise could not be fitted with a Lorentzian component. By contrast, serosal addition of Ba induced a Lorentzian component in the spectrum (5 mM Ba; Fig. 3B). The low-frequency plateau value (S_0) decreased, and the corner frequency (f_c) increased as the serosal Ba concentration was raised stepwise (Fig. 3C).

Inhibition of the macroscopic current by Ba was completely reversible; therefore, we assumed the simplest scheme for channel (R) block, which has also been used by others (e.g., Standen and Stanfield, 1978; Armstrong and Taylor, 1980; Eaton and Brodwick, 1980; Van Driessche and Gögelein, 1980; Vergara and Latorre, 1983; DeCoursey and Hutter, 1984):



As demonstrated previously for amiloride-induced noise (Lindemann and Van Driessche, 1977), if the number of channels at the membrane surface is negligible compared with the concentration of Ba, the overall reaction rate ($1/\tau$) at equilibrium is

$$1/\tau = [\text{Ba}]k_{01} + k_{10} = 2\pi f_c, \quad (5b)$$

and the blocking reaction is pseudo-first order, so that plotting $2\pi f_c$ vs. [blocker] yields a straight line with slope = k_{01} (with units $\text{mM}^{-1} \text{s}^{-1}$) and intercept = k_{10} (in s^{-1}). Fig. 4 shows the relationship between $2\pi f_c$ and serosal [Ba] obtained for locust rectum. The correlation coefficient determined by linear regression was quite high ($r^2 = 0.9965$), although we noticed that the value of $2\pi f_c$ at 3.5 mM Ba was always below the regression line.

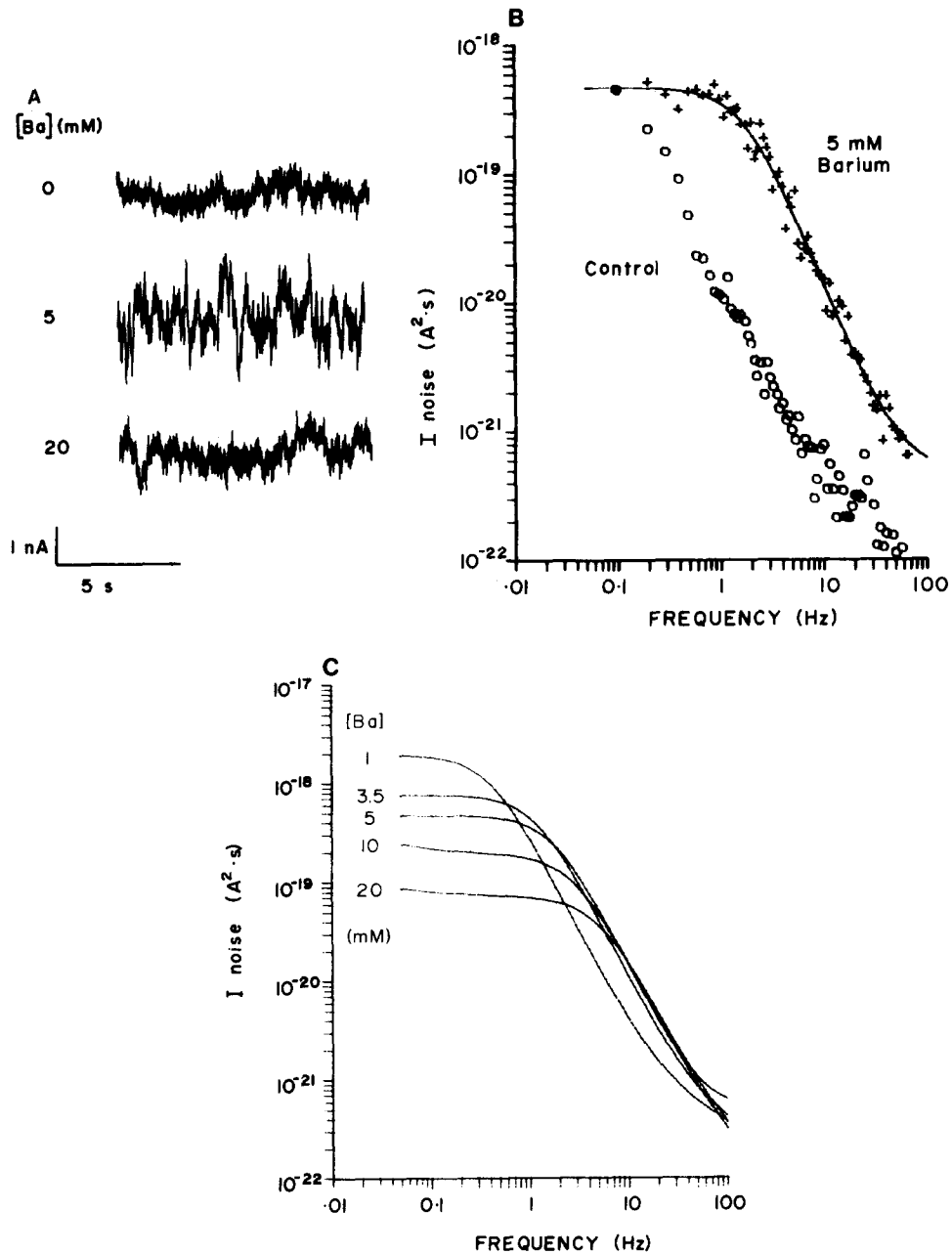


FIGURE 3. Ba-induced fluctuations in I_{sc} . Ba was added to the serosal side in the presence of a serosal-to-mucosal K gradient and 1 mM cAMP. (A) Fluctuations in short-circuit current were measured with 0, 5, or 20 mM Ba on the serosal side. (B) Power spectra obtained in the absence of Ba (○) could not be fitted with a Lorentzian-type function; however, a Lorentzian component was observed after Ba was added to the serosal side (+). (C) Effect of increasing serosal [Ba] on power spectra. Best fits to Eq. 1 are shown at each concentration for one preparation (see text). Preparation LOC0122.

Effect of Ba on the Apparent Single Channel Current

Applying the simplest "on-off" blocking scheme and a two-state kinetic model (e.g., Neher and Stevens, 1977), the low-frequency limit of $S_1(f)$ is

$$S_1(0) = i_{K_{Ba}}^2 M P_o [Ba] k_{01} / \pi^2 f_c^2, \quad (6)$$

where $i_{K_{Ba}}$ is the current flowing through a single (unblocked) channel in the basolateral membrane (see Fig. 1C), M is the number of channels, P_o is the probability that a single channel is unblocked at a particular concentration of Ba, and f_c is the corner frequency of the Lorentzian component at that concentration.

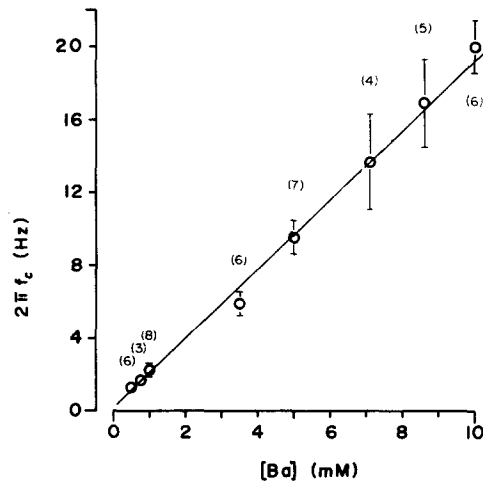


FIGURE 4. Relationship between corner frequency and serosal Ba concentration. Mean \pm SE.

The apparent single channel currents ($i'_{K_{Ba}}$; reasons for the use of "apparent" will become clear in a later section) were calculated for each [Ba] by rearranging Eq. 6 to give

$$i'_{K_{Ba}} = S_1(0) \pi^2 f_c^2 / I_{K_{Ba}} [Ba] k_{01}, \quad (7)$$

and inserting I_K , $S_1(0)$, f_c , and the k_{01} obtained from individual preparations over the entire [Ba] range (0.5–10 mM). Although the single channel current should not depend on Ba concentration, Fig. 5 shows that $i'_{K_{Ba}}$ was approximately eightfold larger at 10 mM [Ba] compared with that at 0.5 mM Ba. The increase in $i'_{K_{Ba}}$ with [Ba] might be explained by several factors: (a) the $2\pi f_c$ -[Ba] plot may not be linear, as evidenced by the low value at 3.5 mM in Fig. 4, (b) attenuation of basolateral membrane current noise by the apical membrane may be reduced at high Ba concentrations, and (c) the driving force for K entry may be enhanced by serosal [Ba].

Re-examination of the $2\pi f_c$ -[Ba] Plot

When data from those five preparations in which f_c was determined at each of the lower Ba concentrations (i.e., 0.5, 1.0, 3.5, and 5.0 mM) were replotted on

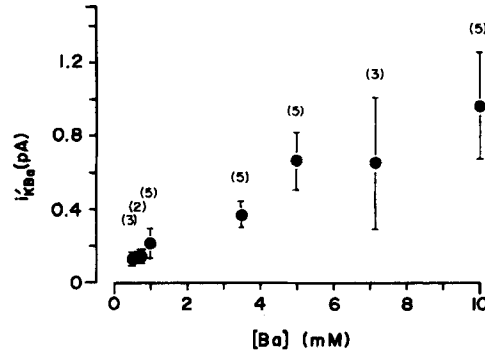


FIGURE 5. Apparent single channel currents ($i'_{K[Ba]}$) calculated for individual preparations at each [Ba] using Eq. 7. $i'_{K[Ba]}$ was about eightfold larger at 10 mM Ba than at 0.5 mM Ba. Mean \pm SE; see also Table I.

an expanded scale, it became obvious that the relationship between $2\pi f_c$ and [Ba] is concave upwards (Fig. 6). If one assumes that Ba interactions in locust K channels are pseudo-first order (as is the case in other preparations: e.g., Van Driessche and Gögelein, 1980; Vergara and Latorre, 1983), then a tangent to the curve at low concentrations would indicate $k_{01} = 0.868 \text{ mM}^{-1} \text{ s}^{-1}$ and $k_{10} = 0.712 \text{ s}^{-1}$. Clearly, this is only an approximation and should overestimate k_{01} and underestimate k_{10} ; nevertheless, the shape of the curve suggests that these errors would be small, and changes in membrane potential are also minimal over this range (see below).

The slope of the $2\pi f_c$ -[Ba] relation was much steeper at high Ba concentrations (5–10 mM; Fig. 4), which is consistent with a value for k_{01} of $\sim 1.94 \text{ mM}^{-1} \text{ s}^{-1}$.

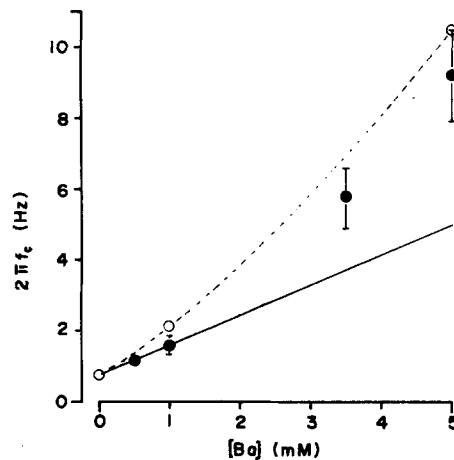


FIGURE 6. Data from five recta in which f_c was obtained in the presence of 0.5, 1.0, 3.5, and 5.0 mM Ba (\circ ; standard error at 0.5 mM Ba was smaller than the symbol). The solid line indicates $k_{01} = 0.868 \text{ mM}^{-1} \text{ s}^{-1}$ and $k_{10} = 0.712 \text{ s}^{-1}$, calculated for a two-state model in which the on and off rate constants are not affected by [Ba]. The open circles were calculated assuming that k_{01} depends on voltage (see Table I), with $k_{01}(0) = 0.378 \text{ mM}^{-1} \text{ s}^{-1}$ and $\gamma = 0.76$. Mean \pm SE.

Although, in principle, it should be possible to calculate k_{10} at high [Ba], the small value of k_{10} and the relatively large extrapolation required to reach the ordinate made this impossible and in fact yielded a small negative value (-0.16 s^{-1}). We believe this is due to the fact that $2\pi f_c$ is dominated by the association rate constant at high blocker concentrations (for example, k_{10} would contribute only $\sim 5\%$ of the $2\pi f_c$ at 10 mM Ba, according to Eq. 5b and Fig. 4). As a consequence, we focus on the Ba association rate constant in the remainder of this paper, reasoning that the large contribution of the on rate constant would make $2\pi f_c$ sensitive to changes in k_{01} .

Effect of Ba on Intracellular Potential

It is well known that Ba is a voltage-dependent blocker in other preparations. The type of curvature in Fig. 6 would be expected if the basolateral membrane potential (V_b) hyperpolarized as the Ba concentration was elevated because this would increase the association rate constant (i.e., the slope). To determine whether Ba addition caused significant hyperpolarization, intracellular potential was measured under the same conditions present during noise measurements (i.e., short-circuited, 1 mM cAMP, transepithelial K gradient, and absence of Cl). Microelectrodes were referenced to either the mucosal or serosal agar bridge and this could be switched while recording from one cell (top of Fig. 7) or between successive impalements (bottom of Fig. 7). Serosal Ba hyperpolarized the basolateral membrane in every preparation, with V_b increasing by 20.7 ± 4.5 mV ($P \ll 0.01$) from -13.8 ± 1.5 to -36.1 ± 12.8 when 10 mM Ba was added (Table I and Fig. 8).

We calculated the voltage dependence of block on the assumption that the curvature in the $2\pi f_c$ -[Ba] relationship results from voltage-dependent association, and that the simplest (single-site, two-barrier) model adequately describes Ba interactions with the channel (Woodhull, 1973). The on rate constant for Ba block (k_{01}) as a function of voltage is then

$$k_{01}(V) = k_{01}(0)\exp(-zF\gamma V/RT), \quad (8)$$

where $k_{01}(0)$ is the association rate constant at $V_b = 0$ mV (in $\text{mM}^{-1} \text{ s}^{-1}$), γ is the fraction of the membrane field sensed by the barrier to Ba entry, and z , F , R , and T have their usual meanings. $k_{01}(0)$ and γ were calculated using Eq. 8 by inserting V_i measured with 1 mM Ba (-13.8 mV; "low potential") or 10 mM Ba (-27.1 mV; "high potential"), and association rate constants for low and high membrane potentials ($k_{01} = 0.868 \text{ mM}^{-1} \text{ s}^{-1}$ at 0.5–1.0 mM Ba; $k_{01} = 1.94 \text{ mM}^{-1} \text{ s}^{-1}$ at 5.0–10.0 mM Ba). The electrical distance of the barrier (γ) was estimated to be 0.76 of the way through the membrane field, and $k_{01}(0)$ was $0.378 \text{ mM}^{-1} \text{ s}^{-1}$. The values of $2\pi f_c$ calculated using these estimates for k_{01} and γ are similar to those observed, although we assumed for simplicity that k_{10} is voltage independent when we made the calculation (broken line, Fig. 6). The agreement might still be improved slightly if k_{10} decreased with hyperpolarization.

Effect of Ba on the Attenuation of Basolateral Current Noise

Short-circuiting the epithelium abolishes V_t , but it does not perfectly voltage-clamp the basolateral membrane, which contains the fluctuating channels. Con-

sequently, transepithelial current noise appears attenuated compared with basolateral conductance fluctuations by some amount that depends on the relative impedance of the apical and basolateral membranes (Van Driessche and Gögelein, 1980; Lindemann and DeFelice, 1981; Wills et al., 1984). When series resistance is much less than R_j , transepithelially measured spectral density, $S_I(f)_{\text{meas}}$, is related to the spectral density under ideal conditions, $S_I(f)$, by

$$S_I(f)_{\text{meas}} = S_I(f) |H(f)|^2, \quad (9)$$

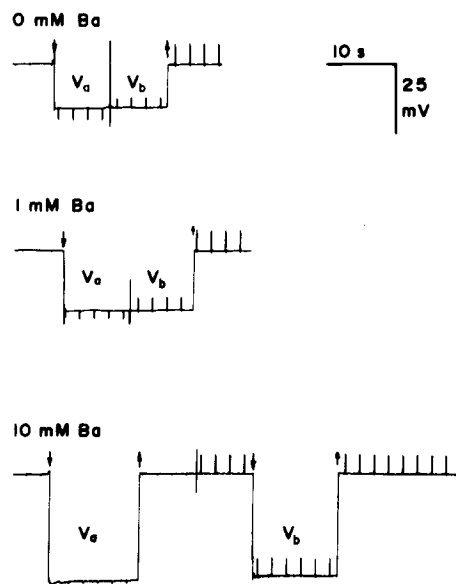


FIGURE 7. Effect of serosal Ba on membrane potentials and relative membrane resistances under short-circuit conditions. cAMP (1 mM) was added to the serosal side and a serosa-to-mucosa K gradient was imposed. Arrows indicate the insertion and retraction of the microelectrodes and transepithelial pulses indicate relative membrane resistances. Deflections in basolateral membrane potential became much larger than those at the apical membrane when Ba was added to the serosal side (compare ΔV_a and ΔV_b at 0 and 10 mM). Preparation LOC1110.

where

$$|H(f)| = \sqrt{(\text{Re}[H(f)])^2 + (\text{Im}[H(f)])^2} \quad (10)$$

and $|H(f)|$ is the modulus of the frequency response function $H(f)$. In principle, the entire noise spectrum should be corrected for this attenuation because it is frequency dependent and might affect estimates of f_c (Lindemann and DeFelice, 1981). However, Ba-induced noise occurs at very low frequencies in this preparation, where membrane capacitance would have little effect. Furthermore, spectra did not show any peaks that would suggest impedance artifacts (Van Driessche and Gögelein, 1980; Van Driessche and Gullentops, 1982). For these reasons, it was sufficient to determine $H(f)$ at the low-frequency limit [i.e.,

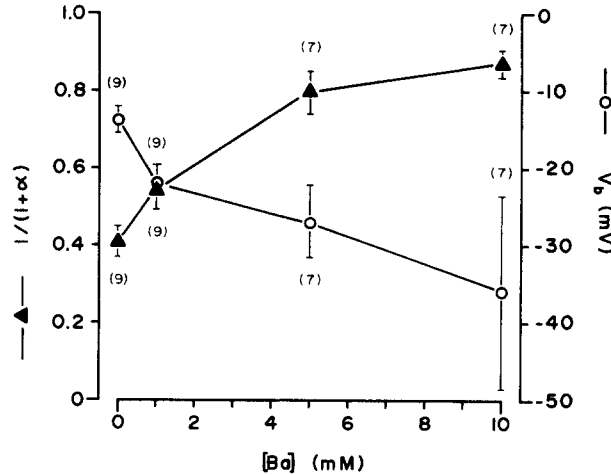


FIGURE 8. Effect of Ba on the fractional resistance of the basolateral membrane [$R_b/(R_a + R_b) \approx 1/(1 + \alpha)$] and basolateral membrane potential (V_b) under I_{sc} conditions. Mean \pm SE.

the plateau value, $S_1(0)$] as

$$|H(0)| = R_b/(R_a + R_b) \approx 1/(1 + \alpha), \quad (11)$$

where α was measured at 0, 1, 5, and 10 mM [Ba] as described in the Methods.

Table I shows that the ratio of apical-to-basolateral membrane resistance (α) declined by $\sim 90\%$ when 10 mM Ba was added to the serosal side, which is consistent with inhibition of most of the basolateral K conductance (Table I). The fractional resistance of the basolateral membrane [$1/(1 + \alpha)$] increased from 0.40 to 0.87 as Ba was added, and the block was half-maximal at ~ 3 mM Ba, which is similar to that observed for inhibition of the macroscopic current during noise experiments. It is clear that adding Ba improves the voltage clamp of the

TABLE I

Effects of Serosal Ba Addition on Intracellular Potential (V_b), Intracellular K Activity (a_k^i), Ratio of Apical to Basolateral Membrane Resistances (α), and Net Electrochemical Potential for K at the Basolateral Membrane ($\Delta\bar{\mu}_k^b/F$)

	Ba concentration			
	0 mM	1.0 mM	5.0 mM	10.0 mM
V_b (mV)	-13.8 ± 1.54 (9)	-22.0 ± 2.41 (9)	-27.1 ± 4.51 (7)	-36.1 ± 12.77 (7)
a_k^i (mM)	57.0 ± 4.0 (8)	58.1 ± 6.5 (7)	62.8 ± 7.1 (6)	62.6 ± 3.6 (5)
α	1.58 ± 0.19 (9)	1.12 ± 0.36 (9)	0.30 ± 0.11 (7)	0.16 ± 0.05 (7)
$\Delta\bar{\mu}_k^b/F$ (mV)	-8.4 ± 3.2 (8)	-13.6 ± 4.8 (7)	-18.4 ± 5.7 (6)	-25.8 ± 4.7 (5)

$\bar{x} \pm SE$ (n = number of tissues).

basolateral membrane, thereby reducing attenuation of the basolateral current fluctuations. Therefore, it is necessary to correct for this effect when calculating i_{KBa} by using the following equation:

$$i_{\text{KBa}} = S_1(0)_{\text{meas}} \pi^2 f_c^2 (1 + \alpha)^2 / I_{\text{KBa}}[\text{Ba}] k_{01}, \quad (12)$$

where $S_1(0)_{\text{meas}}$ is the plateau value for the spectrum of I_{sc} fluctuations.

Effect of Ba on Intracellular K Activity (a_{K}^i) and Net Electrochemical Potential ($\Delta\bar{\mu}_{\text{K}}^b/F$)

It is already clear that serosal Ba addition under these conditions causes V_b to hyperpolarize; however, it was also necessary to measure intracellular K activity at each [Ba], so that the net driving force for K could be determined. Table I shows that Ba had little effect on intracellular K activity (a_{K}^i). It seems likely that intracellular K was maintained by basolateral Na/K-ATPase, so that only minor changes in the net driving force for K entry through the basolateral membrane were attributable to the K gradient (for biochemical and physiological evidence for this enzyme in locust rectum, see Phillips, 1981).

Single Channel i - V Relation

The fact that Ba addition alters i_{KBa} and $\Delta\bar{\mu}_{\text{K}}^b/F$ enabled us to estimate single channel conductance from the relationship between K current and net driving force. Values for k_{01} at low (0.5–1.0 mM) and high (5.0–10.0 mM) Ba concentrations and α , measured at 1 and 10 mM Ba, were inserted into Eq. 12 to obtain i_{KBa} (the single channel current corrected for changes in k_{01} and attenuation). Then i_{KBa} was plotted against the (measured) net driving force for K at 1.0 mM and 10.0 mM [Ba] as shown in Fig. 9. Chord conductance (g_{KBa}) was estimated from the relationship

$$g_{\text{KBa}} = i_{\text{KBa}} / (\Delta\bar{\mu}_{\text{K}}^b/F). \quad (13)$$

Over the narrow range of $\Delta\bar{\mu}_{\text{K}}^b/F$ observed in this study, g_{KBa} was calculated to be ~60 pS. Note that this is only a first estimate because of the variability caused by combining noise and microelectrode data from different tissues. Nevertheless, the estimate is reasonable since the extrapolated reversal for i_{KBa} occurs near electrochemical equilibrium (i.e., $\Delta\bar{\mu}_{\text{K}}^b/F \approx 3$ mV).

Density of Basolateral K Channels

With a simple on-off blocking scheme, the probability that a single channel is unblocked (P_o) is

$$P_o = k_{10} / (k_{01}[\text{Ba}] + k_{10}) = k_{10} / 2\pi f_c. \quad (14)$$

From Eqs. 6 and 14, the number of channels per square centimeter tissue area (i.e., channel density, or M) can be determined as

$$M = I_{\text{KBa}} 2\pi f_c / i_{\text{KBa}} k_{10}. \quad (15)$$

Channel density was calculated using the values for I_{KBa} , i_{KBa} , f_c , and k_{10} from five recta at low [Ba] (0.5–1.0 mM), where k_{10} could be obtained from the $2\pi f_c$ -[Ba] plot. We calculated a density of $178 \pm 17 \times 10^6$ channels/cm².

Locust rectal cells are columnar and the basolateral membrane is extensively infolded. According to electron micrographs (Phillips, J. E., M. S. Jarial, and H. B. Irvine, unpublished observations), the actual area of basolateral membrane is at least 20-fold greater than the macroscopic tissue area. Assuming 20-fold area amplification, we would expect a density of less than one channel per square micron of basolateral membrane, or <200 channels per cell. This estimate is somewhat higher than that deduced for Ca-activated K channels in pancreatic acinar cells (45 ± 11 per cell, obtained by comparing whole cell and single channel current; Maruyama et al., 1983b); however, a greater number of K channels would not be surprising considering the size of locust rectum cells and the importance of K absorption to insect renal function.

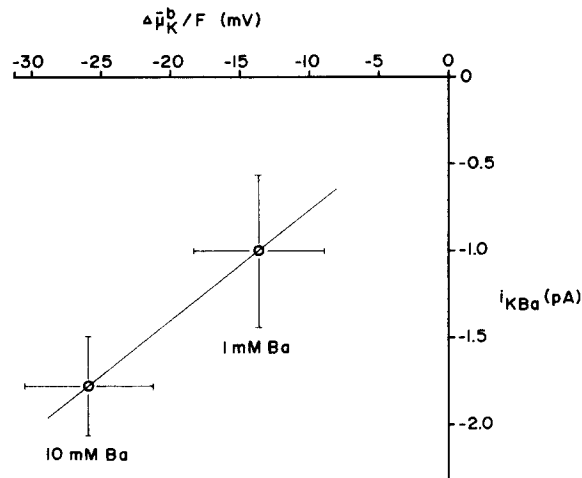


FIGURE 9. Relationship between the net driving force for K across the basolateral membrane and the single channel current obtained by transepithelial fluctuation analysis. Apparent single channel currents in Fig. 5 were corrected for changes in k_{o1} and apical attenuation to obtain i_{KBa} , which was then plotted against net driving force to estimate conductance (60 pS; see text).

DISCUSSION

The locust rectum resembles most tight epithelia by having a significant basolateral membrane K conductance (Hanrahan and Phillips, 1984b). The results described in this paper indicate that the conductance results from Ba-sensitive channels. Using noise analysis and microelectrodes, we obtained evidence that the Ba association rate constant depends on membrane voltage, and the attenuation of transepithelially measured current fluctuations by apical membrane resistance was quantified. After making appropriate corrections for these effects, single channel current and ion-sensitive microelectrode data were used to estimate the conductance and density of basolateral K channels.

Comparison of Single Channel and Basolateral Membrane Conductance

Previous electrophysiological studies of locust rectum were not performed under the conditions used here (i.e., cAMP-stimulated, Cl-free, and high serosal [K]).

However, with the assumption that serosal Ba inhibits only basolateral membrane conductance, we can estimate individual membrane resistances under these conditions by plotting transepithelial conductance (G_t) vs. $\alpha/(1 + \alpha)$ at various Ba concentrations. Junctional and apical membrane conductances can be calculated from the y-intercept and slope, respectively, where

$$G_t = G_j + G_a[\alpha/(1 + \alpha)]. \quad (16)$$

Linear regression of the data at 0, 1, 5, and 10 mM Ba (Figs. 2C and 8) gave a line with $r^2 = 0.983$, slope (G_a) = 3.47 mS cm^{-2} , and intercept (G_j) = 1.25 mS cm^{-2} , from which we calculated $R_b = 182 \text{ } \Omega \text{ cm}^2$ in the absence of Ba. Not surprisingly, this value is lower than that measured previously by cable analysis when serosal [K] was only 10 mM ($429 \text{ } \Omega \text{ cm}^2$; Hanrahan and Phillips, 1984b). R_b increased from 163 to $>1,500 \text{ } \Omega \text{ cm}^2$ when [Ba] was elevated to 10 mM. Paracellular resistance ($R_j = 1/G_j$) is $800 \text{ } \Omega \text{ cm}^2$, which is comparable to that obtained previously using flat-sheet cable analysis of cAMP-stimulated recta bathed with Cl-free saline ($1,047 \text{ } \Omega \text{ cm}^2$; Hanrahan and Phillips, 1984b).

Calculating G_a and G_j in this way assumes that both are unaffected by the addition of Ba to the serosal side. This assumption seems reasonable because 20 mM Ba had no effect on R_t when added to the mucosal side, nor did mucosal Ba affect the I_{sc} or power spectra. A large effect of intracellularly trapped Ba on the apical membrane seems unlikely in view of the dramatic (10-fold) reduction in α caused by adding Ba to the serosal side. Moreover, the apparent voltage dependence of Ba block (i.e., an increase in the on rate after hyperpolarization) would be consistent with block by external but not intracellular Ba.

Do microscopic estimates of single channel conductance and channel density agree with the macroscopic conductance of the basolateral membrane? With a density of 178 million channels/cm² and a single channel conductance of 60 pS (Fig. 8), we would predict the macroscopic K conductance to be $\sim 10.7 \text{ mS cm}^{-2}$. This value is higher than that calculated above ($\sim 5 \text{ mS cm}^{-2}$), but the discrepancy could be explained if the probability of channels being in the open state in the absence of Ba was ~ 0.5 . Noise resulting from rapid, spontaneous fluctuations may have been missed because we did not analyze frequencies above 100 Hz. Using the patch-clamp technique, K channels have been identified in the basolateral membrane of exocrine acinar cells (Maruyama et al., 1983a) and in an absorptive epithelium, rabbit urinary bladder (Hanrahan et al., 1984a). In both preparations, single channel conductance is $\sim 200 \text{ pS}$ when patches are bathed symmetrically by $\sim 150 \text{ mM KCl}$, and spontaneous open-closed transitions are voltage dependent. In rabbit bladder, the open state probability decreases from 0.71 to 0.12 as the membrane is hyperpolarized from -20 to -80 mV . If insect basolateral K channels are similar, it is conceivable that they are open $\sim 50\%$ of the time under the conditions used in this study.

Potential Effects of Ba-insensitive Conductance in the Basolateral Membrane

According to the circuit model in Fig. 1C, all of the Ba-insensitive I_{sc} measured under our experimental conditions must flow through the paracellular pathway. Consequently, the total current through Ba-sensitive channels at any particular [Ba] can be obtained by subtracting the I_{sc} that remains after adding a saturating

dose of Ba (i.e., I_R in Eq. 4). However, if I_R is also comprised of a Ba-insensitive current flowing through the basolateral membrane (e.g., a leak in parallel with the Ba-sensitive channels), then subtraction of I_R would "over-correct" I_{sc} at low blocker concentrations, where the membrane potential, and hence the leak current, would be smaller. We estimated the largest errors in $I_{K_{Ba}}$ ($6 \mu A/cm^2$) and $i_{K_{Ba}}$ (0.14 pA) at 1 mM that could be expected from this effect, although it was necessary for the calculation to assume that Ba-sensitive conductance is completely blocked at 10 mM Ba, so that all the basolateral current is leak at this [Ba]. With this "worst-case" assumption, $g_{K_{Ba}}$ was calculated to be 48 pS using Eq. 13 (vs. 60 pS). Nonetheless, the effect of basolateral leak pathways on our estimate of single channel conductance is probably much less than 12 pS because there is still significant Ba-sensitive current remaining in the presence of 10 mM [Ba] (Figs. 2C and 3C).

Why Does Adding Ba Hyperpolarize the Basolateral Membrane?

Under short-circuit conditions, the apical and basolateral membranes are effectively in parallel, so that the intracellular potential is

$$V_b = E_a R_b / (R_a + R_b) + E_b R_a / (R_a + R_b). \quad (17)$$

K gradients determine E_a and E_b because both membranes are highly K selective under Cl-free conditions (Hanrahan and Phillips, 1984b). It can be seen from Table I that E_b is much smaller (less negative) than E_a because of the presence of high-K saline on the serosal side. According to Eq. 17, increases in R_b caused by the addition of Ba will diminish the contribution of E_b (approximately -5 mV), thereby driving V_b toward E_a (approximately -50 mV). Thus, simple changes in basolateral conductance can account for the hyperpolarization, although some contribution of other factors, such as the Na/K pump, cannot be excluded.

Interpreting the Voltage Dependence of Ba Block

A voltage-induced increase in the Ba association rate constant provides the most straightforward explanation for the curvature in the $2\pi f_c$ -[Ba] plot, and is consistent with findings from other preparations. Nonetheless, three other possible mechanisms should also be mentioned. First, if more than one Ba ion binds to the K channel, the $2\pi f_c$ -[Ba] plot might be described by a power function with a curvature resembling that in Fig. 6. However, it is not obvious why more than one Ba ion would be required to block the pore and other K channels have been shown to bind Ba in a one-to-one manner (e.g., Armstrong et al., 1982; Vergara and Latorre, 1983). A second possibility is that the binding of Ba to one channel might directly increase the affinity of a neighboring channel for Ba independently of membrane voltage. There is no precedent for this type of cooperative block, although it cannot be excluded at this time. A third possibility is that Ba actually passes through the channel so that the increase in $2\pi f_c$ with voltage could be due partly to enhanced entry into the cell (effectively an increase in the off rate). These alternatives, which require more assumptions than our hypothesis of voltage-dependent association, will be tested in the future using single channel methods.

The electrical distance γ of 0.76 suggests that the barrier to externally applied Ba is deep within the membrane electric field. This implies an asymmetrical barrier and suggests that k_{10} should be less voltage dependent than k_{01} . A similar asymmetry has already been shown for block by internal Ba of Ca-activated K channels incorporated into planar bilayers, where the association rate constant from the *cis* side (i.e., cytoplasmic side) depends on voltage ($\gamma = 0.65$) but the dissociation rate constant does not (Vergara and Latorre, 1983).

Under the conditions used in this study, voltage dependence should result in a lowering of the macroscopic K_i for Ba at high concentrations; the affinity of

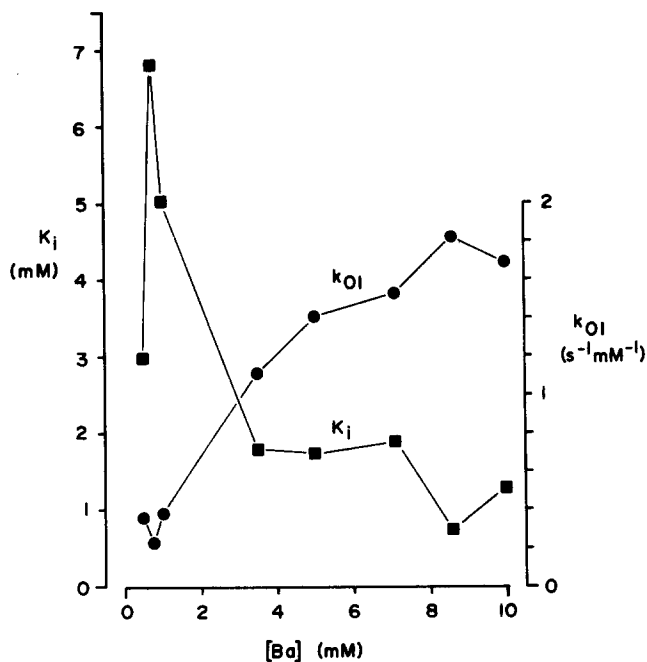


FIGURE 10. K_i (■) and the rate constant for Ba association (●) calculated at each [Ba] from the data shown in Figs. 2C and 4 and the Michaelis-Menten equation $K_i = I_{K_{Ba}}^{max}[Ba]/I_{K_{Ba}} - [Ba]$, assuming $K_i = k_{10}/k_{01}$ and $2\pi f_c = k_{01}[Ba] + k_{10}$.

Ba for the channel should appear to increase as [Ba] is elevated. To test this possibility, K_i was calculated from the mean currents at each [Ba] shown in Fig. 2C, assuming that Ba inhibition is Michaelis-Menten at any particular Ba concentration. Fig. 10 shows that the macroscopic K_i 's generally declined as [Ba] was elevated. Moreover, when K_i and $2\pi f_c$ were used to solve for k_{01} (assuming $K_i = k_{01}/k_{10}$), k_{01} was found to increase with [Ba]. These calculations ignore possible competition between K and Ba (e.g., Sperelakis et al., 1967) but they provide independent evidence that the $2\pi f_c$ -[Ba] curvature can be explained by an increase in k_{01} .

A deep binding site for extracellular Ba has been reported for the delayed rectifier in squid axon ($\gamma = 0.66$, Armstrong et al., 1982) and the inward rectifier in muscle (0.7, Standen and Stanfield, 1978). By contrast, external Ba shows

much weaker voltage dependence in the Ca-activated K channel from rabbit muscle (0.35, Ba on the *trans* side, Vergara and Latorre, 1983). An apparent distinction between these channels is the ability to contain more than one ion. Delayed and inward rectifiers are multi-ion pores (Hodgkin and Keynes, 1955; Hille and Schwarz, 1978), whereas Ca-activated K channels are thought to contain only a single ion (Vergara and Latorre, 1983; but see Latorre et al., 1986). The strong voltage dependence of block by external Ba would seem more consistent with basolateral K channels being multi-ion pores, and we note that Kirk and Dawson (1983) reached the same conclusion from tracer studies of turtle colon basolateral membrane. They observed interactions between "K-like" cations and deviations from Ussing's flux ratio (Ussing, 1949) when transepithelial ^{42}K fluxes were measured after permeabilizing the apical membrane and inhibiting the Na pump. A flux ratio exponent of ~ 2 was obtained, which for a single-file model is related to the number of ions within the channel (Hodgkin and Keynes, 1955; see Heckmann, 1972). Armstrong et al. (1982) have pointed out that the electrical distance for the binding of voltage-dependent blockers such as Ba is probably not unique in multi-ion pores and might be voltage dependent. It is therefore conceivable that the blocking site for Ba may be slightly deeper when the membrane is at the normal potential of -50 mV.

Ba Sensitivity

Since the early demonstration by Pacifico et al. (1969) that serosal Ba inhibits basolateral K conductance in gastric mucosa, evidence for Ba-sensitive permeability has been obtained in at least nine epithelia and the list continues to grow (cf. Lewis et al., 1984b). Sensitivity to serosal Ba appears to be highest in frog skin (Nagel, 1979), intermediate in trachea (Welsh, 1983), and lowest in locust rectum. The concentration required for half-maximal inhibition (K_i) varies between 0.2 and 2.0 mM in these tissues, but this is a reasonable range considering the experimental conditions under which Ba was tested. Different membrane potentials might partly explain the variation, as would different external [K] concentrations: basolateral membrane potential was highest in the frog skin experiments (ranging from -95 to -45 mV after Ba addition), intermediate in trachea (-51 to -28 mV), and lowest in the present study (-8 to -26 mV). We would expect K-Ba competition to have been lowest for frog skin (2.5 mM K), intermediate for trachea (5.4 mM K), and highest in the present study (80 mM K; high-K saline). In comparing Ba inhibition in epithelial and excitable cells, it is interesting that half-maximal block in the millimolar range is similar to findings for delayed rectifiers in frog muscle (0.8 mM Ba; Standen and Stanfield, 1978) and squid axon (3 mM Ba at -70 mV; Armstrong et al., 1982), and also for Ca-activated K channels from rabbit muscle (1.8 mM Ba on *trans* side at 0 mV; Vergara and Latorre, 1983).

Selectivity and Conductance

The ratio $P_{\text{Na}}/P_{\text{K}}$ cannot be estimated reliably from the noise data presented here; however, there is evidence that basolateral K channels are highly selective against Na. First, replacing serosal Na by K (under Cl-free conditions, with K activity elevated approximately sevenfold) caused V_i to hyperpolarize by ~ 50 mV

(Fig. 2A). Second, the net electrochemical driving force for K is normally <4 mV above equilibrium despite high serosal [Na] (i.e., >100 mM; Hanrahan and Phillips, 1984b). Selectivity sequences reported for basolateral K channels generally resemble those of excitable cells: Tl and Rb can both penetrate the basolateral K pathway in turtle colon ($P_{Tl} \approx P_K$, $P_{Rb} = 0.1 P_K$; Kirk and Dawson, 1983). Also, Cs inhibits inward K current at the basolateral membrane of both rabbit colon (Wills et al., 1979) and locust rectum (Hanrahan, J. W., and J. Meredith, unpublished observations).

Locust hindgut K channels appear to have intermediate conductance, lower than many Ca-activated K channels (~180–220 pS in ≥ 100 mM KCl) and the sarcoplasmic reticulum K channel (~120 pS), but higher than delayed and inward rectifiers (2–18 pS, various conditions; see review by Latorre and Miller, 1983). This preliminary estimate of 60 pS for single channel conductance needs to be confirmed eventually using the patch-clamp technique. It is likely that basolateral K channels would have a much larger conductance than 60 pS if they were bathed symmetrically with higher K concentrations as in studies of isolated channels. For comparison, when K channels from sarcoplasmic reticulum are incorporated into lipid bilayers, their conductance is half-maximal in solutions containing 50 mM K activity (Coronado et al., 1980). A similar conductance-activity relationship for locust K channels would result in single channel conductances of ~120 pS when they are bathed symmetrically with 150 mM [K]. Finally, we suspect that locust K channels are Ca insensitive, like those from rabbit urinary bladder, because maneuvers that should drastically alter intracellular [Ca] have no effect on transepithelial conductance (Hanrahan and Phillips, 1985).

We are grateful to Dr. D. Loo for providing a low-noise voltage clamp and to Drs. M. Ifshin and C. Clausen for computer programming. We also thank S. Gopaul for arranging locust shipments and Dr. R. Harrison for the use of his insect room in the Biology Department at Yale.

This work was supported by fellowships from Natural Sciences and Engineering Research Council (NSERC) (Canada) and Medical Research Council to J.W.H., an NSERC grant to J.E.P., and National Institutes of Health grants AM 29962 and AM 33243 to N.K.W. and S.A.L., respectively.

Original version received 13 March 1985 and accepted version received 27 November 1985.

REFERENCES

- Armstrong, C., R. P. Swenson, and S. R. Taylor. 1982. Block of squid axon K^+ channels by internally and externally applied Ba^+ ions. *Journal of General Physiology*. 80:663–682.
- Armstrong, C. M., and S. R. Taylor. 1980. Interaction of barium ions with potassium channels in squid giant axons. *Biophysical Journal*. 30:473–488.
- Brown, K. M., and J. E. Dennis, Jr. 1972. Derivative free analogues of the Levenberg-Marquardt and Gauss algorithms for non-linear least squares approximation. *Numerische Mathematik*. 18:289–297.
- Coronado, R., R. L. Rosenberg, and C. Miller. 1980. Ionic selectivity, saturation, and block in a K^+ -selective channel from sarcoplasmic reticulum. *Journal of General Physiology*. 76:425–446.

- DeCoursey, T. E., and O. F. Hutter. 1984. Potassium current noise induced by barium ions in frog skeletal muscle. *Journal of Physiology*. 349:329–351.
- Eaton, D. C., and M. S. Brodwick. 1980. Effect of barium on the potassium conductance of squid axons. *Journal of General Physiology*. 75:727–750.
- Germann, W. J., and D. C. Dawson. 1984. Two types of potassium channel in the basolateral membrane of the turtle colon. *Biophysical Journal*. 45:302a. (Abstr.)
- Hanrahan, J. W., W. P. Alles, and S. A. Lewis. 1984a. Basolateral anion and K channels from rabbit urinary bladder epithelium. *Journal of General Physiology*. 84:30a. (Abstr.)
- Hanrahan, J. W., J. Meredith, J. E. Phillips, and D. Brandys. 1984b. Methods for the study of transport and control in insect hindgut. In *Measurement of Ion Transport and Metabolic Rate in Insects*. T. J. Bradley and T. A. Miller, editors. Springer-Verlag, New York. 19–67.
- Hanrahan, J. W., and J. E. Phillips. 1984a. KCl transport across an insect epithelium. I. Tracer fluxes and the effects of ion substitutions. *Journal of Membrane Biology*. 80:15–26.
- Hanrahan, J. W., and J. E. Phillips. 1984b. KCl transport across an insect epithelium. II. Electrochemical potentials and electrophysiology. *Journal of Membrane Biology*. 80:27–47.
- Hanrahan, J. W., and J. E. Phillips. 1984c. KCl transport across an insect epithelium. Characterization of K-stimulated Cl absorption and active K transport. *Journal of Experimental Biology*. 111:201–223.
- Hanrahan, J. W., and J. E. Phillips. 1985. Further observations on the regulation of KCl transport across an insect epithelium. *Journal of Experimental Biology*. 116:153–167.
- Hanrahan, J. W., N. K. Wills, and S. A. Lewis. 1983. Barium-induced current fluctuations from the basal membrane of an insect epithelium. *Proceedings of the 29th Congress of the International Union of Physiological Sciences*. 457. (Abstr.)
- Heckmann, K. 1972. Single file diffusion. In *Biomembranes*. F. Kreuzer and J. F. G. Slegers, editors. Plenum Press, New York. 3:127–153.
- Hille, B., and W. Schwarz. 1978. K⁺ channels as multi-ion pores. *Journal of General Physiology*. 72:409–442.
- Hodgkin, A. L., and R. D. Keynes. 1955. The potassium permeability of a giant nerve fibre. *Journal of Physiology*. 128:61–88.
- Kirk, K. L., and D. C. Dawson. 1983. Basolateral potassium channel in turtle colon. Evidence for single-file ion flow. *Journal of General Physiology*. 82:297–314.
- Koefoed-Johnsen, V., and H. H. Ussing. 1958. The nature of the frog skin potential. *Acta Physiologica Scandinavica*. 42:298–308.
- Lapointe, J. Y., J. Cardinal, and R. Laprade. 1984. Characterization of apical membrane ionic permeability of proximal convoluted tubules (PCT). *Kidney International*. 24:307. (Abstr.)
- Latorre, R., and C. Miller. 1983. Conduction and selectivity in K⁺ channels. *Journal of Membrane Biology*. 71:11–30.
- Latorre, R., C. Miller, and G. Eisenman. 1986. The high-conductance Ca⁺⁺-activated K⁺ channel: current-voltage behavior and multi-ion permeation properties. *Biophysical Journal*. 49:576a. (Abstr.)
- Lau, K. R., R. L. Hudson, and S. G. Schultz. 1984. Cell swelling increases a barium-inhibitable potassium conductance in the basolateral membrane of *Necturus* small intestine. *Proceedings of the National Academy of Sciences*. 81:3591–3594.
- Lewis, S. A., A. G. Butt, M. J. Bowler, J. P. Leader, and A. D. C. Macknight. 1984a. Effects of anions on cellular volume and transepithelial Na⁺ transport across toad urinary bladder. *Journal of Membrane Biology*. 83:119–137.
- Lewis, S. A., J. W. Hanrahan, and W. Van Driessche. 1984b. Channels across epithelial cell layers. *Current Topics in Membranes and Transport*. 21:253–293.

- Lewis, S. A., M. S. Ifshin, D. D. F. Loo, and J. M. Diamond. 1984c. Studies of sodium channels in rabbit urinary bladder by noise analysis. *Journal of Membrane Biology*. 80:135–151.
- Lewis, S. A., and J. M. Diamond. 1976. Na⁺ transport by rabbit urinary bladder, a tight epithelium. *Journal of Membrane Biology*. 28:1–40.
- Lindemann, B., and L. J. DeFelice. 1981. On the use of general network functions in the evaluation of noise spectra obtained from epithelia. In *Ion Transport by Epithelia*. S. G. Schultz, editor. Raven Press, New York. 1–13.
- Lindemann, B., and W. Van Driessche. 1977. Sodium-specific membrane channels of frog skin are pores: current fluctuations reveal high turnover. *Science*. 195:292–294.
- Loo, D. D. F., S. A. Lewis, M. S. Ifshin, and J. M. Diamond. 1983. Turnover, membrane insertion, and degradation of sodium channels in rabbit urinary bladder. *Science*. 221:1288–1290.
- Maruyama, Y., D. V. Gallacher, and O. H. Petersen. 1983a. Voltage and Ca⁺-activated K⁺ channel in baso-lateral acinar cell membranes of mammalian salivary glands. *Nature*. 302:827–829.
- Maruyama, Y., O. H. Petersen, P. Flanagan, and G. T. Pearson. 1983b. Quantification of Ca²⁺-activated K⁺ channels under hormonal control in pig pancreas acinar cells. *Nature*. 305:228–232.
- Morgunov, N., and E. L. Boulpaep. 1984. Electrical and chemical analysis of Na/glucose cotransport in isolated perfused *Ambystoma* proximal tubules. *Kidney International*. 24:310. (Abstr.)
- Nagel, W. 1979. Inhibition of potassium conductance by barium in frog epithelium. *Biochimica et Biophysica Acta*. 552:346–357.
- Neher, E., and C. F. Stevens. 1977. Conductance fluctuations and ionic pores in membranes. *Annual Review of Biophysics and Bioengineering*. 6:345–381.
- Pacifico, A. D., M. Schwartz, T. N. MacKrell, S. G. Spangler, S. S. Sanders, and W. S. Rehm. 1969. Reversal by potassium of an effect of barium on the frog gastric mucosa. *American Journal of Physiology*. 216:536–541.
- Phillips, J. E. 1981. Comparative physiology of insect renal function. *American Journal of Physiology*. 241:R241–R257.
- Robinson, R. A., and R. H. Stokes. 1959. *Electrolyte Solutions*. 2nd ed. Butterworths, London. 236.
- Sperelakis, N., M. F. Schneider, and E. J. Harris. 1967. Decreased K conductance produced by Ba in frog sartorius fibers. *Journal of General Physiology*. 50:1565–1583.
- Spring, J. H., and J. E. Phillips. 1980. Studies on locust rectum. II. Identification of specific ion transport processes regulated by corpora cardiacum and cyclic-AMP. *Journal of Experimental Biology*. 86:225–236.
- Standen, N. B., and P. R. Stanfield. 1978. A potential and time-dependent blockade of inward rectification in frog skeletal muscle by barium and strontium ions. *Journal of Physiology*. 280:169–191.
- Ussing, H. H. 1949. The distinction by means of tracers between active transport and tracers. *Acta Physiologica Scandinavica*. 19:43–56.
- Van Driessche, W., and H. Gögelein. 1980. Attenuation of current and voltage noise signals recorded from epithelia. *Journal of Theoretical Biology*. 86:629–648.
- Van Driessche, W., and K. Gullentops. 1982. Conductance fluctuation analysis in epithelia. *Techniques in Cellular Physiology*. P123:1–13.
- Van Driessche, W., and B. Lindemann. 1978. Low noise amplification of voltage and current fluctuations arising in epithelia. *Review of Scientific Instruments*. 49:52–57.

- Van Driessche, W., N. K. Wills, S. D. Hillyard, and W. Zeiske. 1982. K⁺ channels in an epithelial "single membrane" preparation. *Archives Internationales de Physiologie et de Biochimie*. 90:P12-P14. (Abstr.)
- Van Driessche, W., and W. Zeiske. 1980. Ba²⁺-induced fluctuations of potassium channels in the apical membrane of frog skin (*Rana temporaria*). *Journal of Membrane Biology*. 56:31-42.
- Vergara, C., and R. Latorre. 1983. Kinetics of Ca²⁺-activated K⁺ channels from rabbit muscle incorporated into planar bilayers. Evidence for a Ca²⁺ and Ba²⁺ blockade. *Journal of General Physiology*. 82:543-568.
- Welsh, M. J. 1983. Barium inhibition of basolateral membrane potassium conductance in tracheal epithelium. *American Journal of Physiology*. 244:F639-F645.
- Wills, N. K. 1984. Mechanisms of ion transport by the mammalian colon revealed by frequency domain analysis techniques. *Current Topics in Membranes and Transport*. 20:61-85.
- Wills, N. K., W. P. Alles, G. I. Sandle, and H. J. Binder. 1984. Apical membrane properties and amiloride binding kinetics of the human descending colon. *American Journal of Physiology*. 247:G749-G757.
- Wills, N. K., D. C. Eaton, S. A. Lewis, and M. S. Ifshin. 1979. Current-voltage relationship of the basolateral membrane of a tight epithelium. *Biochimica et Biophysica Acta*. 555:519-523.
- Wills, N. K., W. Van Driessche, and W. Zeiske. 1982. Spontaneously fluctuating K⁺ channels in apical and basolateral membranes of the colon. *Biophysical Journal*. 37:280a. (Abstr.)
- Woodhull, A. M. 1973. Ionic blockage of sodium channels in nerve. *Journal of General Physiology*. 61:687-708.